Article

A Transcriptomics-Based Bioinformatics Approach for Identification and In Vitro Screening of FDA-Approved Drugs for Repurposing against Dengue Virus-2

Madhura Punekar [1,†], Bhagyashri Kasabe [2,†], Poonam Patil [1], Mahadeo B. Kakade [1], Deepti Parashar [1], Kalichamy Alagarasu [1,*] and Sarah Cherian [2,*]

1   Dengue & Chikungunya Group, ICMR-National Institute of Virology, 20-A, Dr Ambedkar Road, Pune 411001, Maharashtra, India
2   Bioinformatics Group, ICMR-National Institute of Virology, 20-A, Dr Ambedkar Road, Pune 411001, Maharashtra, India
*   Correspondence: alagarasu@gmail.com (K.A.); sarahcherian100@gmail.com (S.C.)
†   These authors equally contributed to this work.

Abstract: The rising incidence of dengue virus (DENV) infections in the tropical and sub-tropical regions of the world emphasizes the need to identify effective therapeutic drugs against the disease. Repurposing of drugs has emerged as a novel concept to combat pathogens. In this study, we employed a transcriptomics-based bioinformatics approach for drug identification against DENV. Gene expression omnibus datasets from patients with different grades of dengue disease severity and healthy controls were used to identify differentially expressed genes in dengue cases, which were then applied to the query tool of Connectivity Map to identify the inverse gene–disease–drug relationship. A total of sixteen identified drugs were investigated for their prophylactic, virucidal, and therapeutic effects against DENV. Focus-forming unit assay and quantitative RT-PCR were used to evaluate the antiviral activity. Results revealed that five compounds, viz., resveratrol, doxorubicin, lomibuvir, elvitegravir, and enalaprilat, have significant anti-DENV activity. Further, molecular docking studies showed that these drugs can interact with a variety of protein targets of DENV, including the glycoprotein, the NS5 RdRp, NS2B-NS3 protease, and NS5 methyltransferase The in vitro and in silico results, therefore, reveal that these drugs have the ability to decrease DENV-2 production, suggesting that these drugs or their derivatives could be attempted as therapeutic agents against DENV infections.

Keywords: repurposing drugs; DENV-2; dengue fever; antiviral therapy; FDA-approved drugs

1. Introduction

Dengue fever (DF) and dengue haemorrhagic fever are mosquito-borne diseases caused by the dengue virus serotype (DENV-1, 2, 3, and 4) [1]. The incidence of DENV has grown dramatically around the world in recent decades. The World Health Organization (WHO) estimates 390 million dengue infections per year in 128 countries [2]. In the tropics and subtropics, dengue is one of the most common diseases, which is a public health concern. DENV, a positive-strand RNA virus, is a member of the family Flaviviridae and genus flavivirus, transmitted by *Aedes aegypti* and *Ae. albopictus* mosquitoes [3]. The DENV infection usually causes dengue fever (DF) with flu-like illness, and DF occasionally evolves into a potentially lethal complication termed severe dengue (SD), which is characterized by plasma leakage, fluid accumulation, respiratory distress, and severe bleeding [4].

To date, there is no treatment or approved antivirals available for DENV. The only available methods are mosquito-control strategies which prevent the transmission of the virus, and hence, there is an urgent need to design better medications for treating dengue viral infection. The traditional drug discovery procedure is more expensive, can take many

years, and requires unending work to find a novel drug. This problem can be overcome by drug repurposing or drug repositioning, which involves a drug discovery strategy for the United States Food and Drug Administration (FDA)-approved drugs [5]. Among the many approaches employed to identify drugs to treat dengue, drug repurposing has gained popularity, which is safer and more economic. The targeted drugs have further been tested for their effectiveness against other diseases and proven safe for treatment of the human diseases [5]. In recent years, drug repurposing has been applied in many studies to identify treatments [6–8]. Antidiabetic, anticholesteremic, antihistamine, antipsychotic, antibiotic, antiparasitic, and antimalarial drugs have been repurposed to assess their effectiveness against DENV infection [5,9]. These studies helped uncover potential drug targets for improving DENV therapy.

In this study, we applied computational drug-repurposing methods by using publicly available gene expression data for gene–disease–drug analysis. The differentially expressed genes were inputted to the connectivity map (CMap) server to identify drug candidates for DENV. The identified candidate drugs were tested in vitro for anti-DENV activity. The drugs with antiviral activity were further investigated for their ability to interact with DENV proteins using molecular docking analysis.

2. Materials and Methods

The schematic representation of the in silico as well as in vitro study workflow is shown in Figure 1.
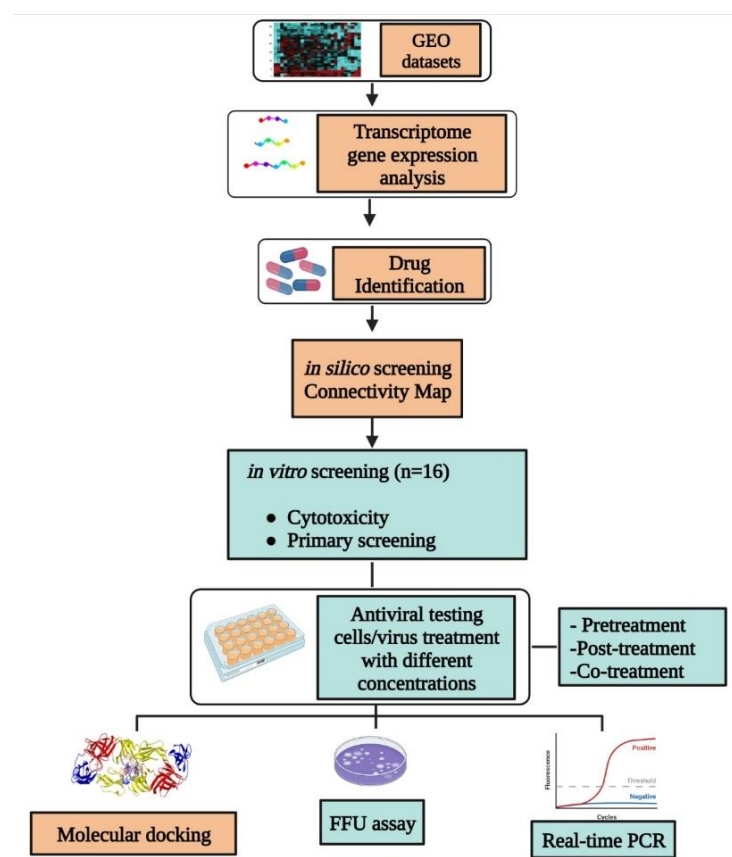

Figure 1. In silico and in vitro methods used for selecting and studying the antiviral activity of drugs for repurposing.

2.1. Transcriptome Data Collection and Analysis

Identification of differential gene expression between dengue patients and healthy individuals.

Several transcriptomic studies (microarray and RNASeq) were referred for the expression analysis of dengue virus infection in host cells. Three microarray gene expression datasets based on whole blood samples of dengue-infected humans were downloaded from the GEO database as follows: GSE18090 [10] from blood samples of eight healthy and ten DHF patients, GSE51808 [11] from nine healthy and ten DHF patients, and GSE84331 [12] from five healthy and three DHF patients. For each dataset, the gene signature profiles were obtained by considering an adjusted p (Adj. p)-value < 0.05 in the test between healthy and DHF patients by the z-score transformation of the three GEO matrices.

2.2. Identification of Drug Candidates Using CMap

CMap is a collection of genome-wide transcriptional expression data from human cell lines that have been treated with chemical compounds [13]. Simple pattern matching algorithms together enable the discovery of decisive functional connections between drugs, genes, and diseases through the transitory feature of common gene expression changes. The CMap has a library containing over 1.5 million gene expression profiles from ~5000 small-molecule compounds and ~3000 genetic reagents, tested in multiple cell types. The query tool on the clue.io site helps in identifying perturbens that give rise to similar (or opposing) gene signatures [14]. In drug repositioning for dengue, the differentially expressed signature profiles between healthy individuals and DHF patients were applied to the query tool to identify inverse drug–disease relationships. The threshold of significance for each drug was set at $p < 0.1$ using the permutated results. Once queried, the results were accessible, and the heat map result of the connections was viewed. In the heat map, the liver cell line was selected as HEPG2 and the perturben type was selected as a compound. Thereafter the potential therapeutic candidates were identified among the compounds with the highest (negative) connectivity score. Connectivity scores less than −90 were considered significant according to Connectopedia, the Clue knowledge database.

2.3. Cells and Virus

The Vero CCL-81 (ATCC® CCL 81™) cell line, originally derived from the African green monkey kidney, was used to assess antiviral activity. These cells were cultured at 37 °C and under 5% CO_2 in Minimal Essential Medium (MEM), (HiMedia®, Mumbai, India) with 10% foetal bovine serum (FBS) (Gibco™, Grand Island, NY, USA) and antimycotic antibiotic solution (Sigma Aldrich®, St. Louis, MO, USA). The DENV-2 virus (Strain No. 803347) was used in this study and a 0.1 Multiplicity of Infection (MOI) was used for infection.

2.4. Stock Preparation of Compounds

The drugs procured from Sigma Aldrich, St. Louis, MO, USA, (Table 1) were included in this study. The 20 mM stock solutions of the drugs were prepared using dimethyl sulfoxide (DMSO, 100%) as a diluent. The stock solutions were stored at −20 °C for further analysis.

Table 1. Profile of the drugs repurposed as DENV-2 inhibitors.

Sr. No.	Compound Name	Pharmacological Class	CC$_{50}$ Value (µM)	Reported Activity
1.	Temsirolimus	Antineoplastic	12.24	1. Antineoplastic [15,16] 2. Antiviral, anti-SARS-CoV-2, and anti-HBV [17,18]
2.	Doxorubicin hydrochloride	Antineoplastic	116.9	1. Antineoplastic [19] 2. Antiviral [20–24]
3.	2-Fluoroadenine-9-β-D-arabinofuranoside	Antineoplastic	42.24	1. Antineoplastic [25] 2. Immunosuppressant [26]
4.	Retinoic acid p-hydroxyanilide	Antineoplastic	2.38	1. Antineoplastic [27]

Table 1. *Cont.*

Sr. No.	Compound Name	Pharmacological Class	CC$_{50}$ Value (μM)	Reported Activity
5.	Docetaxel	Antineoplastic	2.26	1. Antineoplastic [28,29] 2. Antiviral-EBV [30]
6.	Evodiamine	Antineoplastic	10.24	1. Antineoplastic [31,32] 2. Anti-inflammatory [33] 3. Antiviral [34–36], viral, and bacterial pneumonia [37]
7.	Staurosporine from Streptomyces sp.	Antibiotic	0.08	1. Antineoplastic [38,39] 2. Antimicrobial [40]
8.	Resveratrol	Anti-inflammatory	40.82	1. Antilipemic and antidiabetic [41] 2. Anti-inflammatory [42,43] 3. Antineoplastic [44] 4. Alzheimer's disease pathomechanism modulator [45] 5. Antioxidant and antimicrobial [46] 6. Antiviral [47] 7. Cardioprotective [48]
9.	Metyrapone	Adrenal steroid synthesis inhibitor	19,554	1. 11β-hydroxylase enzyme inhibitor [49] 2. Antidepressant [50]
10.	(+)-JQ1	Bromodomain inhibitor (Thienotriazolodi-azepine)	0.82	1. Bromodomain inhibitor [51] 2. Reduces IFN-γ expression [52] 3. Antineoplastic [53,54] 4. Cardioprotective [55,56] 5. Anti-inflammatory [57]
11.	Givinostat hydrochloride hydrate	Hydroxamate inhibitor	1.61	1. Anti-inflammatory [58] 2. Cardioprotective [59] 3. Antineoplastic/antiangiogenic [60]
12.	Thapsigargin	Calcium channel blocker	1.38	1. Antineoplastic [61] 2. Endoplasmic reticulum Ca^{2+} inhibitor [62] 3. Antiviral [63,64]
13.	Enalaprilat	Angiotensin-converting enzyme (ACE) inhibitor	80.83	1. Treatment of hypertension and hypertensive heart failure [65]
14.	5α-Androstan-3β-ol	Steroid	23.13	No reported activity
15.	Elvitegravir	Antiviral	12.7	1. Antiretroviral [66,67]
16.	Lomibuvir	Antiviral	38.54	1. Anti-HCV activity [68,69] 2. SARS-CoV-2 [70]

2.5. Cytotoxicity Screening of Compounds

The cytotoxicity screening of the drugs was performed using a 3-(4,5-dimethythiazol-2-yl)-2,5-diphenyl tetrazolium bromide (MTT) assay as described in a previous study [71]. The Vero CCL-81 cells cultured in a 96-microtitre-well plate with a density of 2×10^4 cells per well were used with 80% confluency. The compound concentrations were prepared using MEM without antibiotics and with 2% foetal bovine serum (FBS) as the diluent, and a twofold dilution technique (200 to 0.78 μM) was adopted.

The cells were then incubated with these drugs in different microtiter plates for five days (120 h) at 37 °C with 5% CO_2, and further incubated with MTT solution (5 mg/mL) for three hours at 37 °C. A microplate reader (BioTek Synergy, Santa Clara, CA, USA) was used to measure the solubilized formazan crystals at 570 nm with a reference filter of 690 nm. Further, we computed the percentage viability of the cells at different concentrations of the drug in comparison with cell control, and CC$_{50}$ values of the drugs were calculated using non-linear regression analysis using GraphPad Prism software version 7.

2.6. Antiviral Assay

For screening, the maximum non-toxic concentration of the drugs was selected for the assessment of antiviral activity before infection (pre-treatment), during infection (co-treatment), and after infection (post-treatment). For all three treatments, 5×10^4 cells/well were used with 0.1 multiplicity of infection (MOI) of DENV-2. After infection, the cells

were washed twice to remove unbound virus particles and the plates were incubated for five days as per the treatment condition.

Pre-treatment condition involved incubation of the drug onto the cells for 24 h prior to infection. For post-treatment, the cells were infected with the virus for one hour and treated with the drug for five days. In the case of co-treatment, the virus and drug mixture were incubated for one hour and later this mixture was added to the cells and incubated for one hour, followed by the washing step and incubation of five days.

The viral genomic RNA and infectious virus particle titre of cell culture supernatants taken from separate wells treated with different concentrations were analysed using real-time RT-PCR and focus-forming unit (FFU) assay.

Drugs which showed anti-DENV activity were again tested for their anti-DENV activity at different concentrations ≤ maximum non-toxic dose to find out the minimal dose that exerts antiviral activity. The same treatment condition under which the drug showed activity was used for these dose-dependent studies. A virus control (VC) in which cells were infected but not treated was also maintained. The experiments were performed in triplicate at three independent time points.

2.7. Focus Forming Unit Assay and Real-Time RT-PCR

For the quantification of virus particles, FFU assay was used. The assay was performed in a 96-well plate as described earlier [72,73]. Approximately 2×10^4 cells/well were seeded in a 96-well plate and incubated for 24 h. Tenfold serial dilutions of the culture supernatants were added to the cells and the plates were incubated for one hour. After incubation, MEM with 2% FBS and 1.8% carboxymethyl cellulose was added and incubated at 37 °C for five days in a CO_2 incubator. After incubation, cells were washed with phosphate-buffered saline (PBS) containing Tween 20 detergent and fixed with chilled acetone and methanol (1:1 ratio). A blocking buffer (1% bovine serum albumin dissolved in PBS) was added and incubated for 40 min at 37 °C. Later, the washing step was again performed, and the cells were incubated with primary antibody (anti-prM-dengue antibody with a dilution of 1:200) for 40 min, followed by the addition of secondary antibody (anti-mouse IgG HRP conjugate with a dilution of 1:1000) and incubated for 40 min. After every addition, a washing step was performed. The last step involved the addition of substrate (True Blue Peroxidase Substrate by KPL) in dark, followed by incubation at room temperature for 15 min. The substrate was removed after the blue tinge formation and dried before counting the number of foci. The virus titre was determined by counting the number of foci.

Quantitative real-time RT-PCR (qRT-PCR) for estimating the copy number of DENV-2 was performed as described earlier [72,73]. A QIAmp Viral RNA mini kit (Qiagen, Hilden, Germany) was used for the extraction of viral RNA. One-step qRT-PCR using a commercial kit (SuperScript III One-Step RT-PCR System with Platinum Taq DNA Polymerase; ThermoFisher Scientific, Waltham, MA, USA) (Invitrogen SuperScript III Platinum One-step qRT-PCR Kit, Waltham, MA, USA) was used for the detection and quantification of RNA. Oligonucleotide sequences were used as described earlier [72,73]. The amplification conditions included incubation at 50 °C for 30 min, followed by 95 °C for 10 min, and 40 cycles of 95 °C for 15 s and 60 °C for one minute. The copy numbers were calculated based on a standard graph generated using Ct values of tenfold dilutions of in vitro-transcribed viral RNA with known copy numbers. The assays were repeated for the compounds which showed inhibitory activity compared to the virus control.

2.8. Statistical Analysis

The virus output was expressed as $\log_{10}$ mean viral RNA copies/mL or $\log_{10}$ mean FFU/mL. One-way ANOVA with correction for multiple comparisons was used to compare the test conditions to the VC. A *p*-value less than 0.05 was considered significant. All analysis was performed using GraphPad Prism software version 7 (GraphPad software, San Diego, CA, USA).

2.9. Molecular Docking Studies with DENV Protein Targets

The Schrödinger Drug Discovery Suite was used for protein preparation and docking calculations (2020-3). The two-dimensional structures of all the compounds were retrieved from PubChem [74]. All DENV-2 three-dimensional (3D) crystallographic target protein structures including envelope glycoprotein (1OKE.pdb), DENV-2 non-structural proteins including NS2B-NS3 protease (4M9K.pdb), NS5 methyltransferase (MTase) domain (1R6A.pdb), and NS5 RdRp (RNA dependent RNA Polymerase) domain structure (5ZQK.pdb) were retrieved from the Protein Data Bank (PDB) [75] (https://www.rcsb.org/ (accessed on 15 June 2022). The protein structure was prepared (pre-processed, optimized, and minimized) using the protein preparation wizard in Maestro v. 12.5 [76]. The compound structures were prepared by the LigPrep module of Maestro v. 12.5 [76,77]. Grid-based molecular docking was used to help the compounds bind in multiple potential conformations. The hydronation and tautomeric modes of the amino acids were adjusted to match a pH of 7.2. The receptor grid-generating module of Maestro v.12.5 was used to generate the grid. A scaling factor of 1.0, and 0.25 Å, partial charge cut-off for van der Waals radius were applied.

The detergent binding pocket (β-D-glucoside β-OG) of the envelope protein was used as the active site [78] as this pocket is identified as a potential site for small-molecule fusion inhibitors against the envelope protein. Further, the allosteric site pocket for NS2B-NS3 protease [79], conserved motifs, and priming loop for NS5 RdRp domain [80], as well as the site map-generated pocket that was used for NS5 methyltransferase domain, were selected for the molecular docking protocol. The drug binding site was predicted through the site map module of Maestro v.12.5 (Schrödinger, New York, NY, USA).

The docking was carried out using SP/XP (Standard/extra precision) mode [76,77]. The study of DENV-2 protein binding interactions and ligand flexibility was carried out using Glide molecular docking. The binding energies were measured in kcal/mol. The BIOVIA Discovery Studio 2020 client software suite was used to analyse interactions and visualise molecules of docked complexes of all the DENV target crystal structures. The compounds with the highest binding scores and strong interaction profiles were supposed to be the most active compounds against the target receptor protein. The crystal structure was later refined and optimized for further docking procedures.

3. Results

3.1. Transcriptomic Analysis

Using the GSE18090 dataset, we identified 31 signature genes (4 upregulated and 27 downregulated) with significant differences in expression between the DHF patients and the 8 healthy controls. Additionally, we identified 3858 (148 upregulated and 3710 downregulated) and 1941 (541 upregulated and 1400 downregulated) differentially expressed genes in the GSE51808 and GSE84331 datasets, respectively. The genes were filtered out based on the cut-off criteria of adj. p-value < 0.015 and log fold change >2. After combining the signature genes from all three GEO datasets, 1585 signature genes were obtained (Table S1).

3.2. CMap Analysis

The list of the top 300 upregulated/downregulated signature genes from the three datasets that were compatible with the HG-U133A platform of CMap, was used to query the clue.io CMap system. The valid list of differentially expressed genes from the three datasets was queried on CMap for the drug candidates and hits with significant inverse gene signatures (connectivity score < −90) were shortlisted. There were a total of 200 significant drugs (Table S2) obtained with statistical significance ($p < 0.1$). This includes different groups such as CDK inhibitors, JAK inhibitors, interferons, angiogenesis inhibitors, and HDAC inhibitors (Figure 2).
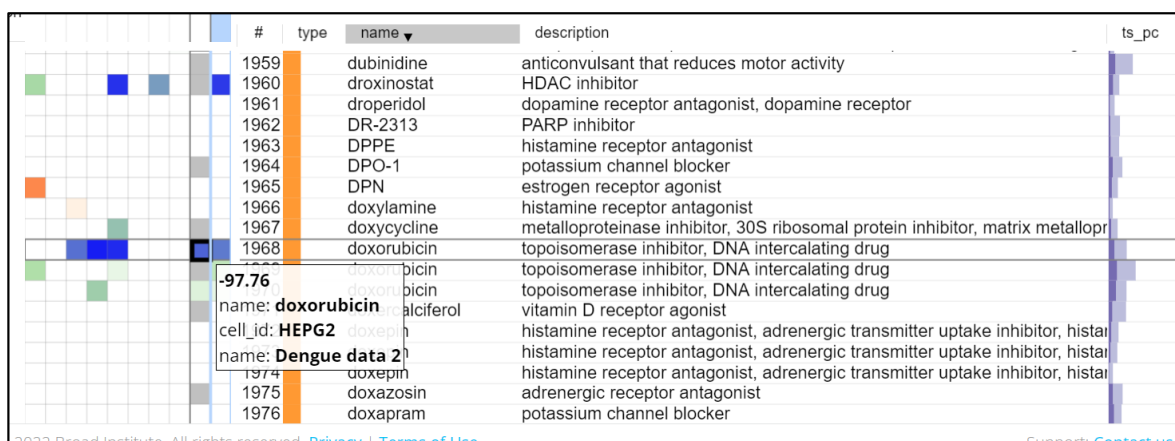
#	type	name ▾	description	ts_pc
1959		dubinidine	anticonvulsant that reduces motor activity	
1960		droxinostat	HDAC inhibitor	
1961		droperidol	dopamine receptor antagonist, dopamine receptor	
1962		DR-2313	PARP inhibitor	
1963		DPPE	histamine receptor antagonist	
1964		DPO-1	potassium channel blocker	
1965		DPN	estrogen receptor agonist	
1966		doxylamine	histamine receptor antagonist	
1967		doxycycline	metalloproteinase inhibitor, 30S ribosomal protein inhibitor, matrix metallopr	
1968		doxorubicin	topoisomerase inhibitor, DNA intercalating drug	
		doxorubicin	topoisomerase inhibitor, DNA intercalating drug	
		doxorubicin	topoisomerase inhibitor, DNA intercalating drug	
		alciferol	vitamin D receptor agonist	
		doxepin	histamine receptor antagonist, adrenergic transmitter uptake inhibitor, histar	
		doxepin	histamine receptor antagonist, adrenergic transmitter uptake inhibitor, histar	
1974		doxepin	histamine receptor antagonist, adrenergic transmitter uptake inhibitor, histar	
1975		doxazosin	adrenergic receptor antagonist	
1976		doxapram	potassium channel blocker	

-97.76
name: **doxorubicin**
cell_id: **HEPG2**
name: **Dengue data 2**

Support: Contact us

Figure 2. Snapshot of the heat map generated by querying the DHF DEGs in CMap. The blue coloured gradient indicates the negative connectivity score of the compounds with inverse gene signatures.

3.3. Viral Targeting Drugs Identified for Repurposing against DENV

Among the list of drug compounds identified by CMap analysis, some are direct viral targeting such as flavivirus RNA polymerase inhibitor, protease inhibitor, etc., while others are host targeting such as histone deacetylase (HDAC) inhibitor. In this study, 16 of these drug compounds were tested for their antiviral efficacy against DENV-2 and evaluated. The profile of these compounds is listed in Table 1.

3.4. Cytotoxicity Evaluation of Compounds

The cell viability of all the drugs (*n* = 16) was tested using an MTT assay in Vero CCL-81 cells. The CC_{50} values of all the drugs are provided in Table 1. Seven drugs were highly toxic. The concentration of the drug which allowed approximately 80% cell viability was further used for studying the antiviral activity. In Figure S1, the impact of different drugs at various concentrations on cell viability is shown with CC_{50} values.

3.5. Primary Antiviral Screening of Compounds against DENV-2

The drugs were tested for their antiviral activity under three circumstances (Figure 3a–c), i.e., pre-treatment (prophylactic), co-treatment (virucidal), and post-treatment (therapeutic). Focus-forming unit (FFU) assay was used to quantify the virus particles. Out of 16 compounds, five compounds (doxorubicin, resveratrol, lomibuvir, elvitegravir, and enalaprilat), showed antiviral activity (≥1.0 log10 reduction compared with virus control) against DENV-2 under different treatment settings. Three drugs, i.e., resveratrol and lomibuvir, had both prophylactic and therapeutic antiviral activity against DENV-2. Elvitegravir had only prophylactic antiviral activity against DENV-2. Doxorubicin had both virucidal and therapeutic antiviral activity against DENV-2. Enalaprilat had only therapeutic antiviral activity against DENV-2 (Table 2). As a result, these drugs were selected for further exploration in a dose-dependent manner, as well as in in silico experiments to determine their target specificity.

3.6. Dose-Dependent Antiviral Effect of Repurposed Drugs against DENV

Dose-dependent antiviral effect of effective drugs, i.e., doxorubicin, resveratrol, lomibuvir, elvitegravir, and enalaprilat, on DENV-2 was examined under different treatment settings and concentrations. The effective drugs were categorised under three treatment settings: prophylactic, therapeutic, and virucidal.
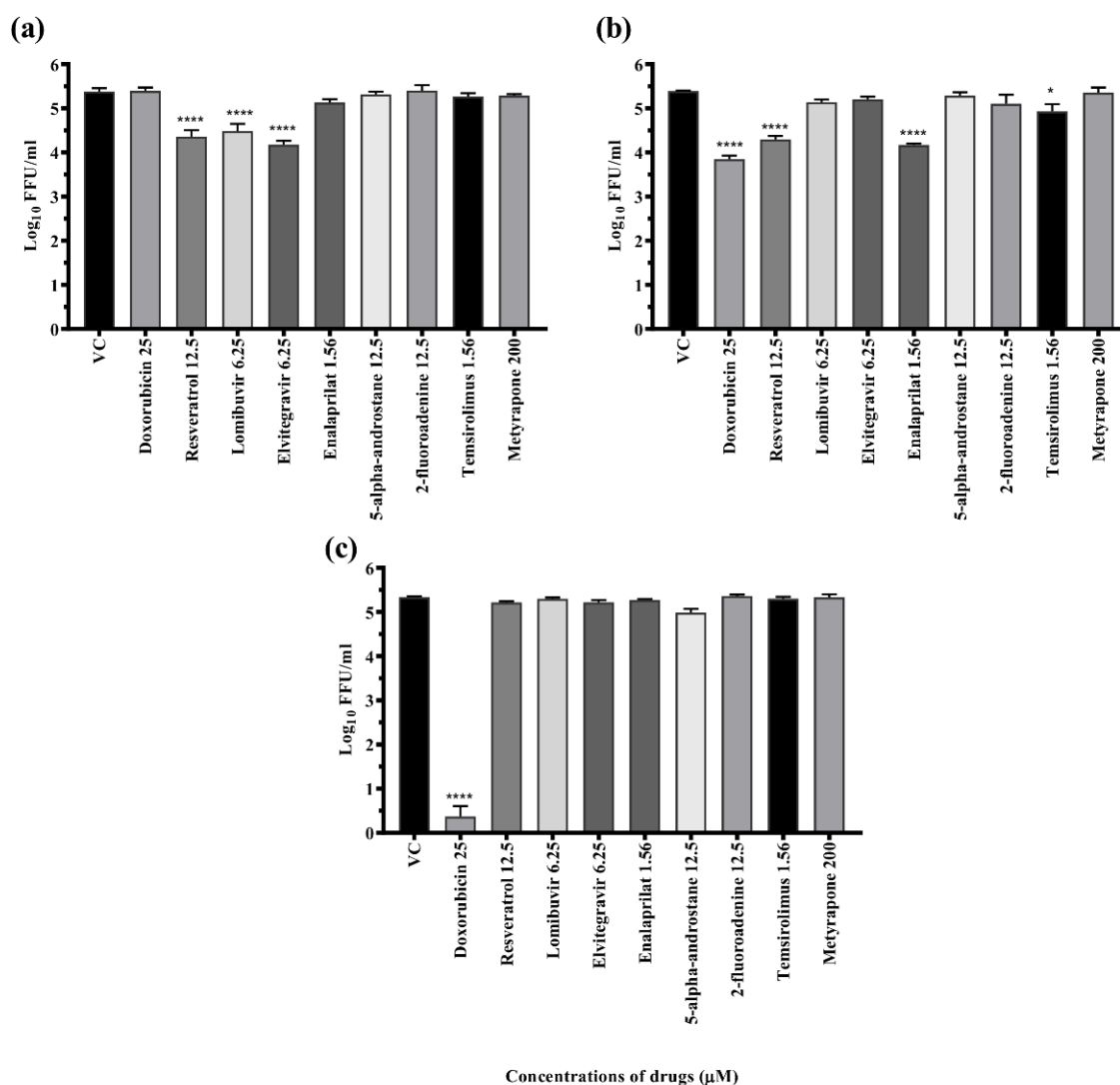
Figure 3. Antiviral screening of drugs for repurposing at maximal nontoxic concentration against DENV under (**a**) pre-, (**b**) post-, and (**c**) co-treatment conditions. Vero CCL-81 cells were treated with a maximum non-toxic dose of drugs for 24 h in a pre-, co-, and post-infection manner and incubated for 120 h with DENV. Post incubation, plates were frozen and culture filtrates were used for different assays. Experiments were performed in triplicate in two independent trials. Results were plotted based on mean log10 of focus-forming unit/mL $\pm$ standard error. All the treatment groups were compared with a control group (VC) (infected cells without treatment). **** $p < 0.0001$, * $p < 0.05$.

Table 2. Summary of effective inhibition under different treatment conditions.

Sr. No.	Compound Name	Chemical Structure	CC50 (μM)	Maximum Concentration (μM)	Log Difference Effectiveness against DENV-2	EC50 (μM)	Selectivity Index (SI)
1	Doxorubicin		116.9	25	Post-treatment—1.453 Co-treatment—4.958	19.99 6.573	5.848 17.785
				12.5	Co-treatment—4.377	6.573	17.785
				6.25	Co-treatment—2.107	6.573	16.115
2	Resveratrol		40.54	12.5	Post-treatment—1.226 Pre-treatment—1.188	4.013 7.592	10.102 5.340
				6.25	Post-treatment—1.115	4.013	10.102
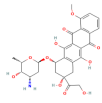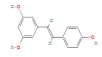
Table 2. *Cont.*

Sr. No.	Compound Name	Chemical Structure	CC50 (μM)	Maximum Concentration (μM)	Log Difference Effectiveness against DENV-2	EC50 (μM)	Selectivity Index (SI)
3	Enalaprilat		80.83	1.56	Post-treatment—1.239	1.079	74.911
4	Elvitegravir		12.7	6.25	Pre-treatment—1.316	4.405	2.883
5	Lomibuvir		38.54	6.25	Pre-treatment—1.224	3.740	10.305
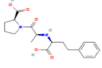
3.6.1. Drugs Exerting Prophylactic Effects

Resveratrol: The pre-treatment of cells with 12.5 μM resveratrol showed >1 $\log_{10}$ reduction ($p < 0.0001$) in the virus titre compared to VC (5.445 to 4.257 mean $\log_{10}$ FFU/mL) (Figure 4). Resveratrol treatment did not result in a significant reduction in the $\log_{10}$ titre of viral RNA copy number (Figure S2).
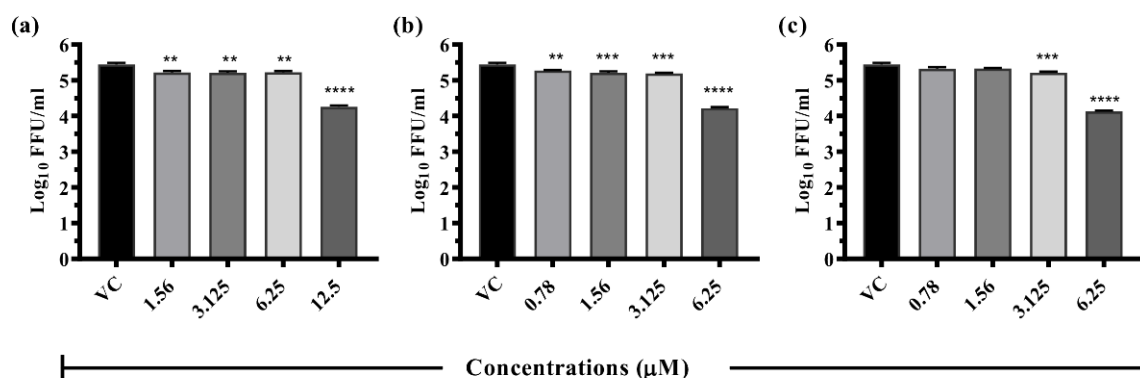
Figure 4. Antiviral effects of resveratrol, lomibuvir, and elvitegravir against DENV under pretreatment condition. Vero CCL-81 cells were treated with different concentrations of respective drugs for 24 hrs and infected with DENV-2 and incubated for 120 h. The cultured filtrates were used for the FFU assay: (**a**)—resveratrol, (**b**)—lomibuvir, and (**c**)—elvitegravir. Experiments were performed in triplicate at three independent time points. Results were plotted based on mean $\log_{10}$ of focus-forming unit/mL $\pm$ standard error. All the treatment groups were compared with a virus control (VC) group (infected cells which did not receive drugs). **** $p < 0.0001$, *** $p < 0.0005$, ** $p < 0.01$.

Lomibuvir: Under pre-treatment conditions, lomibuvir exerted one log reduction in virus titre (5.445 to 4.221 mean $\log_{10}$ FFU/mL) at 6.25 μM concentration (Figure 4). Quantitative real-time RT-PCR results revealed that the drug did not affect viral RNA titre under pre-treatment condition (Figure S2).

Elvitegravir: This drug at 6.25 μM concentration of the drug showed a reduction from 5.445 (VC) to 4.129 mean $\log_{10}$ FFU/mL (Figure 4) but there was no reduction in the case of viral RNA titre (Figure S2).

3.6.2. Drugs Exerting Therapeutic Effects

Doxorubicin: A substantial reduction in virus foci (5.424 to 3.971 mean $\log_{10}$ FFU/mL value) was detected in cells which received post infection treatment with a 25 μM concentration of drug ($p < 0.0001$) (Figure 5). The drug did not result in a significant reduction in the $\log_{10}$ titre of viral RNA copy number under post-treatment condition (Figure S2).
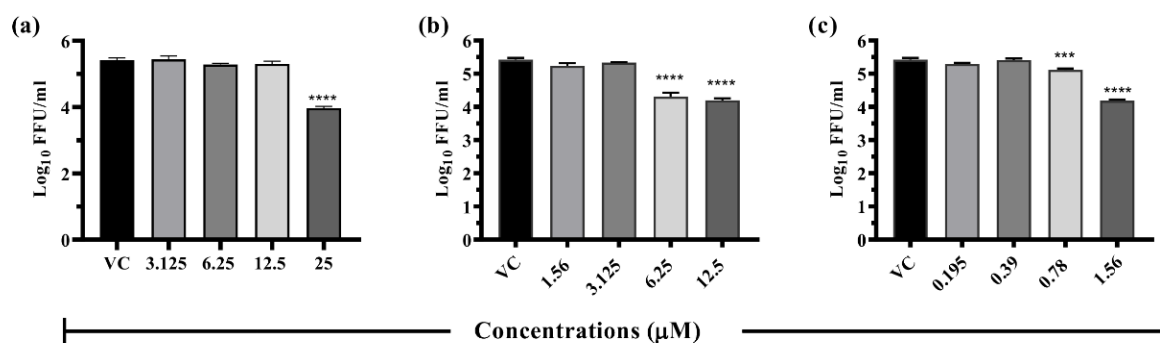
Figure 5. Antiviral effects of doxorubicin, resveratrol, and enalaprilat against DENV under post-treatment conditions. Vero CCL-81 cells were administered the drug at different concentrations immediately after infection and incubated for 120 h after infection. The cultured filtrates were used for the FFU assay: (**a**)—doxorubicin, (**b**)—resveratrol, and (**c**)—enalaprilat. Experiments were performed in triplicate at three independent time points. Results were plotted based on mean log10 of focus-forming unit/mL $\pm$ standard error. All the treatment groups were compared with a virus control (VC) group (infected cells which did not receive drugs). **** $p < 0.0001$, *** $p < 0.0005$.

Resveratrol: Resveratrol at 12.5 µM and 6.25 µM concentrations showed ≥ 1 $\log_{10}$ reduction (5.424 to 4.198 mean $\log_{10}$ FFU/mL) ($p < 0.0001$) of the virus titre compared to VC (Figure 5). There was no significant reduction observed in the $\log_{10}$ titre of viral RNA copy number (Figure S2).

Enalaprilat: This drug showed more than one log reduction in the case of post-treatment (5.424 to 4.184 mean $\log_{10}$ FFU/mL) at 1.56µM concentration (Figure 5). However, the post-treatment condition did not show a corresponding reduction in viral RNA titre. (Figure S2).

3.6.3. Drugs Exerting Virucidal Effects

Doxorubicin: A detailed study was performed with different concentrations (25 µM, 12.5 µM, 6.25 µM, and 3.125 µM) of doxorubicin and the co-treatment of cells with 25 µM concentration showed ~100% reduction (~5 $\log_{10}$) ($p < 0.0001$); at 12.5 µM ($p < 0.0001$) and 6.25 µM, the virus titre showed a difference of ~2 $\log_{10}$FFU titre ($p < 0.0001$) when compared with VC (Figure 6). A significant 4 $\log_{10}$ titre ($p < 0.0001$) decrease in RNA copy number of DENV-2 was observed for co-treatment at 25 µM, whereas a ~3 $\log_{10}$ reduction was observed at 12.5 µM ($p < 0.0001$) and 6.25 µM ($p < 0.0001$) concentrations (Figure S2).

3.7. Effect of Different Drugs on the Percent Cell Viability of the Infected Cells

To rule out that the anti-DENV activity exerted by different drugs was not due to cell death, the cells were cultured in 96-well plates, infected, and treated with a maximum non-toxic dose of the drugs which exerted anti-DENV activity under different treatment conditions. In one set of experiments, cells were incubated for three days after incubation while in another set cells were incubated for five days. After incubation, an MTT assay was performed and the percent cell viability in each well was calculated using viability in cell control (uninfected and untreated cells) as reference. The results revealed that irrespective of days and the treatment condition, the percent cell viability was greater for infected cells which received treatment compared with infected cells which did not receive treatment (virus control) (Figure 7a–c). The only exception was enalaprilat for which the percent cell viability was not different compared to VC (Figure 7b). This proved that the increase in percent cell viability was due to drug treatment which inhibited the virus replication and subsequent cytopathic effect.
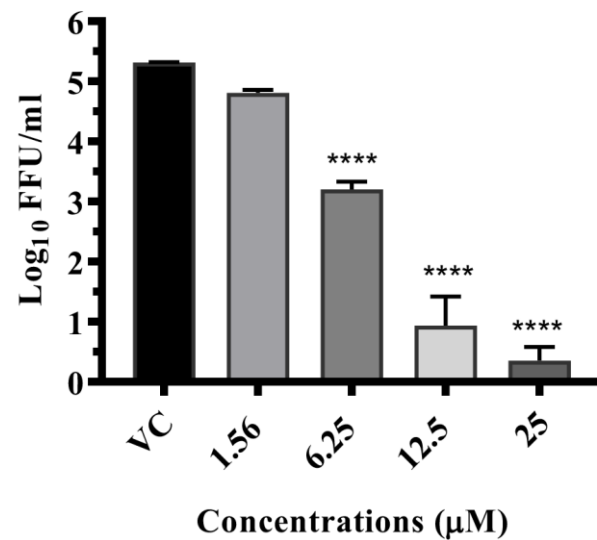
Figure 6. Antiviral effects of doxorubicin under co-treatment condition. The virus was treated with doxorubicin at different concentrations and the virus drug mixture was used for infection. Infected Vero CCL-81 cells were incubated for 120 h after infection. The culture filtrates were used for the FFU assay. Experiments were performed in triplicate at three independent time points. Results were plotted as mean log10 of focus-forming unit/mL ± standard error. All the treatment groups were compared with a virus control (VC) group (infected cells which did not receive drugs). **** $p < 0.0001$.
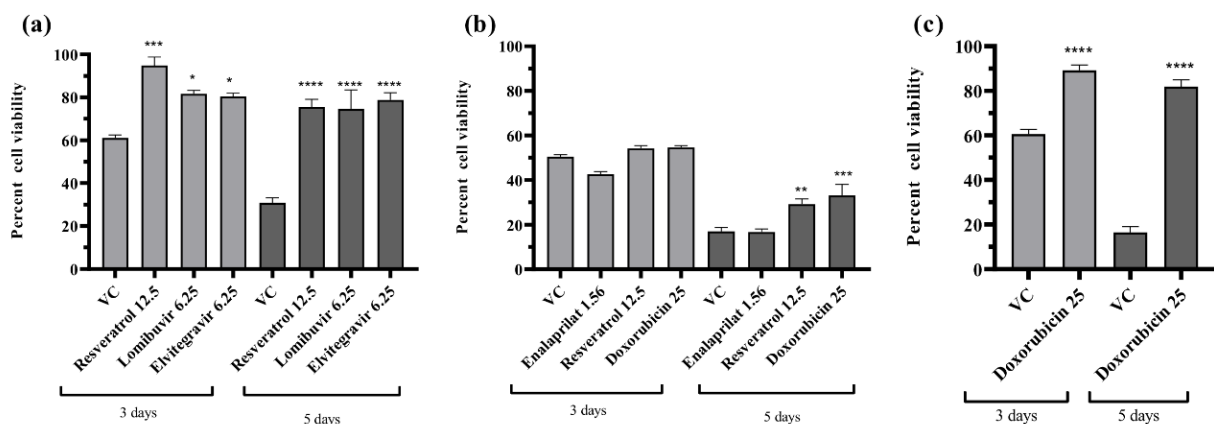
Figure 7. Effect of various drugs on the percent cell viability of the infected cells under different treatment conditions. (**a**)—pre-treatment, (**b**)—post-treatment, and (**c**)—co-treatment. **** $p < 0.0001$, *** $p \leq 0.0005$, ** $p < 0.01$, * $p < 0.05$.

3.8. In Silico Interaction Studies of the Select Drugs with DENV Protein Targets

To explore the potential mode of action of the drugs resveratrol, doxorubicin, lomibuvir, elvitegravir, and enalaprilat, computational molecular docking studies were performed with DENV targets using Schrödinger's Glide. Following the docking procedure, the best pose was chosen based on conformation and docking energy. The scoring function algorithm implemented in Schrodinger was used to compute the binding affinity in terms of the docking score.

Among the different DENV targets, the docking interaction of doxorubicin was found to be the best with DENV E protein (Figure 8e) which exhibited that doxorubicin docked with a strong binding affinity of −5.8 kcal/mol. The doxorubicin interaction involves two conventional hydrogen bonds, four pi-alkyl, and a single pi-sulphur interaction. The residues THR 236, PRO 217, ALA 263, and MET 260 were involved in the above interactions.
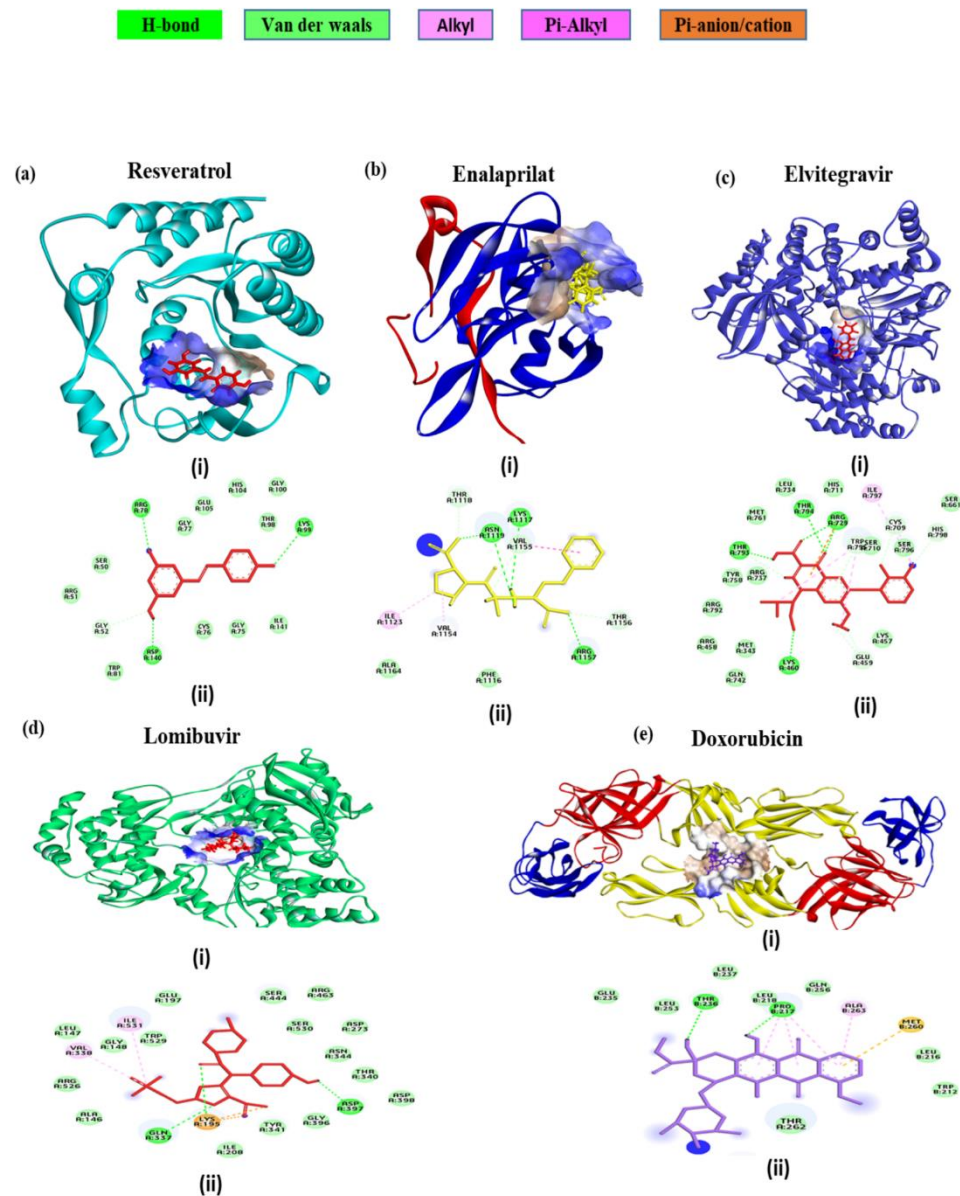
Figure 8. Molecular docking interaction of five repurposed drugs with DENV structural and nonstructural proteins. Ribbon diagram with the solvent surface rendered view (probe radius 1.4 Å) and 2-dimensional interaction diagram showing interaction with DENV: (**a**) NS5 methyltransferase domain, (**b**) NS2B-NS3 protease domain, (**c**) NS5 RdRp domain, (**d**) NS5 RdRp domain, and (**e**) Envelope glycoprotein complex. (i)—3D interaction diagram, (ii)—2D interaction diagram.

The docking interaction analysis of resveratrol was found to be optimal with the DENV NS5 MTase domain (Figure 8a). The binding affinity was found to be −5.7 kcal/mol and residues ARG78, LYS99, and ASP 140 made three hydrogen bonds, indicating that resveratrol can make a stable complex with the DENV MTase domain.

The DENV NS2B-NS3 protease is one of the most prominent targets for anti-DENV inhibitors. Aside from the main catalytic location (HIS51, ASP75, and SER135), a specific allosteric binding site is also present, which has been previously suggested for noncompetitive inhibitors. The enalaprilat docking results (Figure 8b) showed that it interacted with allosteric site residues of DENV NS2B-NS3 protease with a binding affinity of −3.02 kcal/mol. A total of seven interactions were formed: four hydrogen bonds formed with allosteric site residues VAL1155, ASN1119, ARG1157, and LYS1117 and three hydrophobic interactions formed with VAL1155, ILE1123 and VAL1154. These in-

teractions reveal that enalaprilat could have inhibiting activity at the allosteric site of NS2B-NS3 protease.

Examining the docking contact of elvitegravir with the NS5 RdRp domain (Figure 8c) highlighted a binding affinity of −5.27 kcal/mol. The potential binding site of elvitegravir was close to the catalytic site showing interactions with the residues of all the three conserved motifs (Q598-N614, G662-D664, and C709-R729) as well as residues of the priming loop (H786-M809). The molecular interactions displayed two hydrogen bonds formed by ARG729 and the hydroxyl group of elvitegravir. Also, three other hydrogen bonds were formed with THR794, THR 793, and LYS460. A single pi-cation interaction was noted with ARG729. There were multiple numbers of hydrophobic interactions, including alkyl and pi-alkyl bonds with ILE797, TRP795, and SER710.

The docking interaction study of lomibuvir with the DENV RdRp domain (Figure 8d) revealed a strong binding affinity of −4.9 kcal/mol. The molecular non-bonded interaction analysis displays that there were three hydrogen bonds with LYS195, GLN337, and ASP 397, two alkyl bonds with ILE531, VAL338, one salt bridge with LYS195, and one electrostatic bond with LYS 195.

4. Discussion

Dengue fever has been a serious public health problem in tropical and sub-tropical areas around the world and the only preventive measure available for the dengue virus is the control of mosquitoes. The development of effective and safe dengue virus vaccines is still a challenging topic because of antibody-dependent enhancement (ADE) [81]. ADE accounts for the severity of secondary infections that develop in the form of dengue haemorrhagic fever (DHF) and dengue shock syndrome [82]. Among the four serotypes of DENV, DENV-2 significantly causes more severity in patients than the other three serotypes [83]. Since there is no cure for DENV, repurposing known compounds could be a life-saving consequence for the majority of the world's population. Several studies report anti-DENV activity using repurposed compounds [5,84–87].

In this study, we incorporated different classes of drugs including antineoplastic, anti-inflammatory, antibiotics, adrenal steroid synthesis inhibitors, antiviral, steroids, neuromuscular blockers, calcium channel blockers, enzyme inhibitors, hydroxamate inhibitors, and bromodomain inhibitors as shortlisted from a transcriptomics-based approach.

Among the five drugs (resveratrol, doxorubicin, lomibuvir, elvitegravir, and enalaprilat) which showed antiviral activity, doxorubicin, resveratrol, and enalaprilat were the only drugs which showed maximum inhibition of DENV-2 in vitro under the post-treatment condition. Resveratrol is a naturally occurring polyphenol, which is known to exhibit anti-inflammatory, antineoplastic, anti-diabetic, antilipemic, antioxidant, antimicrobial, as well as antiviral activity [41–44,46,47,85]. The other activities include a cardioprotective mechanism and a modulator of Alzheimer's disease [45,48]. The docking analysis revealed that resveratrol interacted with the DENV NS5 MTase domain and formed a stable complex with it and might account for the antiviral activity of the drug. An earlier study reported that resveratrol inhibited DENV-2 in Huh-7 cells but at a higher concentration in the range of 50–100 μM [88]. Resveratrol has been shown to inhibit DENV-2 infection in HEK293T/17 cells at concentrations from 25 to 50 μM [88]. In the present study, we have demonstrated the anti-DENV activity at lower concentrations (in the range of 6.25–12.5 μM). Resveratrol also inhibits the translocation of high mobility group box 1 protein from the nucleus to the cytoplasm and also increased the expression of interferon-stimulated genes in DENV-infected Huh-7 cells [88]. Thus, resveratrol might confer an antiviral state and may act as a prophylactic as well as a therapeutic agent.

Doxorubicin, an anthracycline antibiotic, isolated from *Streptomyces peucetius var. caesius*, exhibits antineoplastic activity by intercalating between DNA base pairs [19]. Many studies have reported that doxorubicin can inhibit a variety of viruses including herpes simplex virus, HIV, enterovirus, hepatitis C virus (HCV), and SARS-CoV-2 [20–23]. An in vitro study by Kaptein et al. reported that doxorubicin and its derivatives inhibit the flavivirus

replication cycle [24]. In the present study, doxorubicin exerted both virucidal as well as a therapeutic effect against DENV-2. In silico studies revealed that doxorubicin may interact with the E protein and binds specifically to the hydrophobic pocket in which residues of the fusion peptide are also accommodated [73]. It is conceivable that doxorubicin may interact with the DENV envelope protein preventing its binding to the host cell receptor. The main limitation posed by doxorubicin concerns the reports of its cardiotoxicity induced by long-term doxorubicin exposure [89]. The structure of doxorubicin might provide clues to the synthesis of derivatives and molecules which can bind to DENV E protein with high affinity but with no cardiotoxic effects.

Enalaprilat, an angiotensin-converting enzyme (ACE) inhibitor, is an active metabolite of enalapril prodrug and is used for the treatment of hypertension, heart failure, and chronic renal diseases. Enalaprilat is known to inhibit the conversion of angiotensin I to angiotensin II by acting antagonistically against the angiotensin-converting enzyme (ACE) [90]. Enalaprilat exerted therapeutic antiviral activity against DENV-2. Enalaprilat interacted with DENV NS2B-NS3 protease at the proposed allosteric binding site for non-competitive inhibition, though with a low binding affinity. It is possible that enalaprilat can affect the DENV protease activity and contribute to the inhibition of DENV. Angiotensin II inhibitors, by acting either on the angiotensin II receptor or ACE, have been shown to inhibit DENV and Zika virus [91,92]. Enalaprilat might modulate the host response and contribute to virus inhibition.

Lomibuvir is a non-nucleoside polymerase inhibitor, belonging to the thiophene carboxylic acid group. It is used in the treatment of chronic HCV infection, and the mechanism involves binding to the thumb pocket 2 of the HCV NS5B polymerase [68,69]. Elvitegravir was the first HIV-1 inhibitor approved by the Food and Drug Administration (FDA) in 2012. It acts as an integrase strand transfer inhibitor for HIV-1 [66,67]. In silico studies revealed that both drugs interacted with the DENV NS5 RdRp domain. However, the in silico results are not supported by in vitro results since both lomibuvir and elvitegravir showed prophylactic activity against DENV infection but no therapeutic activity. It is possible that both these drugs can bind to host receptors and prevent binding of DENV or might induce an antiviral state contributing to inhibition of DENV infection. Further studies are needed to confirm the same.

Overall, in this study, we have identified five potential drugs that can be repurposed as DENV therapeutics. In vivo validation studies would further help in consolidating the findings and facilitate clinical trials.

References

1. Gubler, D.J. Dengue and Dengue Hemorrhagic Fever. *Clin. Microbiol. Rev.* **1998**, *11*, 480–496. [CrossRef] [PubMed]
2. Dengue and Severe Dengue. Available online: https://www.who.int/news-room/fact-sheets/detail/dengue-and-severe-dengue (accessed on 17 January 2022).
3. Murugesan, A.; Manoharan, M. Dengue Virus. *Emerg. Reemerging Viral Pathog.* **2020**, *1*, 281–359. [CrossRef]
4. De Almeida, R.R.; Paim, B.; de Oliveira, S.A.; Souza, A.S.; Gomes, A.C.P.; Escuissato, D.L.; Zanetti, G.; Marchiori, E. Dengue Hemorrhagic Fever: A State-of-the-Art Review Focused in Pulmonary Involvement. *Lung* **2017**, *195*, 389–395. [CrossRef] [PubMed]
5. Botta, L.; Rivara, M.; Zuliani, V.; Radi, M. Drug Repurposing Approaches to Fight Dengue Virus Infection and Related Diseases. *Front. Biosci. Landmark Ed.* **2018**, *23*, 997–1019. [CrossRef] [PubMed]
6. Rudrapal, M.; Khairnar, S.J.; Jadhav, A.G. *Drug Repurposing (DR): An Emerging Approach in Drug Discovery*; IntechOpen: London, UK, 2020; ISBN 978-1-83968-521-7.
7. Sultana, J.; Crisafulli, S.; Gabbay, F.; Lynn, E.; Shakir, S.; Trifirò, G. Challenges for Drug Repurposing in the COVID-19 Pandemic Era. *Front. Pharmacol.* **2020**, *11*, 588654. [CrossRef]
8. Sleigh, S.H.; Barton, C.L. Repurposing Strategies for Therapeutics. *Pharm. Med.* **2010**, *24*, 151–159. [CrossRef]
9. Low, Z.Y.; Farouk, I.A.; Lal, S.K. Drug Repositioning: New Approaches and Future Prospects for Life-Debilitating Diseases and the COVID-19 Pandemic Outbreak. *Viruses* **2020**, *12*, 1058. [CrossRef]
10. Nascimento, E.J.M.; Braga-Neto, U.; Calzavara-Silva, C.E.; Gomes, A.L.V.; Abath, F.G.C.; Brito, C.A.A.; Cordeiro, M.T.; Silva, A.M.; Magalhães, C.; Andrade, R.; et al. Gene Expression Profiling during Early Acute Febrile Stage of Dengue Infection Can Predict the Disease Outcome. *PLoS ONE* **2009**, *4*, e7892. [CrossRef]
11. Soares-Schanoski, A.; Baptista Cruz, N.; de Castro-Jorge, L.A.; de Carvalho, R.V.H.; Santos, C.A.D.; da Rós, N.; Oliveira, Ú.; Costa, D.D.; Santos, C.L.S.D.; Cunha, M.D.P.; et al. Systems Analysis of Subjects Acutely Infected with the Chikungunya Virus. *PLoS Pathog.* **2019**, *15*, e1007880. [CrossRef]
12. Chandele, A.; Sewatanon, J.; Gunisetty, S.; Singla, M.; Onlamoon, N.; Akondy, R.S.; Kissick, H.T.; Nayak, K.; Reddy, E.S.; Kalam, H.; et al. Characterization of Human CD8 T Cell Responses in Dengue Virus-Infected Patients from India. *J. Virol.* **2016**, *90*, 11259–11278. [CrossRef]
13. Lamb, J.; Crawford, E.D.; Peck, D.; Modell, J.W.; Blat, I.C.; Wrobel, M.J.; Lerner, J.; Brunet, J.-P.; Subramanian, A.; Ross, K.N.; et al. The Connectivity Map: Using Gene-Expression Signatures to Connect Small Molecules, Genes, and Disease. *Science* **2006**, *313*, 1929–1935. [CrossRef] [PubMed]
14. Lamb, J. The Connectivity Map: A New Tool for Biomedical Research. *Nat. Rev. Cancer* **2007**, *7*, 54–60. [CrossRef] [PubMed]
15. Bufalo, D.D.; Ciuffreda, L.; Trisciuoglio, D.; Desideri, M.; Cognetti, F.; Zupi, G.; Milella, M. Antiangiogenic Potential of the Mammalian Target of Rapamycin Inhibitor Temsirolimus. *Cancer Res.* **2006**, *66*, 5549–5554. [CrossRef] [PubMed]
16. Bellmunt, J.; Szczylik, C.; Feingold, J.; Strahs, A.; Berkenblit, A. Temsirolimus Safety Profile and Management of Toxic Effects in Patients with Advanced Renal Cell Carcinoma and Poor Prognostic Features. *Ann. Oncol.* **2008**, *19*, 1387–1392. [CrossRef] [PubMed]
17. Mullen, P.J.; Garcia, G.; Purkayastha, A.; Matulionis, N.; Schmid, E.W.; Momcilovic, M.; Sen, C.; Langerman, J.; Ramaiah, A.; Shackelford, D.B.; et al. SARS-CoV-2 Infection Rewires Host Cell Metabolism and Is Potentially Susceptible to MTORC1 Inhibition. *Nat. Commun.* **2021**, *12*, 1876. [CrossRef]
18. Saso, W.; Tsukuda, S.; Ohashi, H.; Fukano, K.; Morishita, R.; Matsunaga, S.; Ohki, M.; Ryo, A.; Park, S.-Y.; Suzuki, R.; et al. A New Strategy to Identify Hepatitis B Virus Entry Inhibitors by AlphaScreen Technology Targeting the Envelope-Receptor Interaction. *Biochem. Biophys. Res. Commun.* **2018**, *501*, 374–379. [CrossRef] [PubMed]
19. Tacar, O.; Sriamornsak, P.; Dass, C.R. Doxorubicin: An Update on Anticancer Molecular Action, Toxicity and Novel Drug Delivery Systems. *J. Pharm. Pharmacol.* **2012**, *65*, 157–170. [CrossRef]
20. Coelmont, L.; Kaptein, S.; Paeshuyse, J.; Vliegen, I.; Dumont, J.-M.; Vuagniaux, G.; Neyts, J. Debio 025, a Cyclophilin Binding Molecule, Is Highly Efficient in Clearing Hepatitis C Virus (HCV) Replicon-Containing Cells when Used Alone or in Combination with Specifically Targeted Antiviral Therapy for HCV (STAT-C) Inhibitors. *Antimicrob. Agents Chemother.* **2009**, *53*, 967–976. [CrossRef]
21. De Palma, A.M.; Heggermont, W.; Leyssen, P.; Pürstinger, G.; Wimmer, E.; De Clercq, E.; Rao, A.; Monforte, A.-M.; Chimirri, A.; Neyts, J. Anti-Enterovirus Activity and Structure-Activity Relationship of a Series of 2,6-Dihalophenyl-Substituted 1H,3H-Thiazolo[3,4-a]Benzimidazoles. *Biochem. Biophys. Res. Commun.* **2007**, *353*, 628–632. [CrossRef]
22. Johansson, S.; Goldenberg, D.M.; Griffiths, G.L.; Wahren, B.; Hinkula, J. Elimination of HIV-1 Infection by Treatment with a Doxorubicin-Conjugated Anti-Envelope Antibody. *AIDS* **2006**, *20*, 1911–1915. [CrossRef]

23. Al-Motawa, M.S.; Abbas, H.; Wijten, P.; de la Fuente, A.; Xue, M.; Rabbani, N.; Thornalley, P.J. Vulnerabilities of the SARS-CoV-2 Virus to Proteotoxicity—Opportunity for Repurposed Chemotherapy of COVID-19 Infection. *Front. Pharmacol.* **2020**, *11*, 585408. [CrossRef] [PubMed]
24. Kaptein, S.J.F.; Burghgraeve, T.D.; Froeyen, M.; Pastorino, B.; Alen, M.M.F.; Mondotte, J.A.; Herdewijn, P.; Jacobs, M.; de Lamballerie, X.; Schols, D.; et al. A Derivate of the Antibiotic Doxorubicin Is a Selective Inhibitor of Dengue and Yellow Fever Virus Replication In Vitro. *Antimicrob. Agents Chemother.* **2010**, *54*, 5269–5280. [CrossRef] [PubMed]
25. Rai, K.R.; Peterson, B.L.; Appelbaum, F.R.; Kolitz, J.; Elias, L.; Shepherd, L.; Hines, J.; Threatte, G.A.; Larson, R.A.; Cheson, B.D.; et al. Fludarabine Compared with Chlorambucil as Primary Therapy for Chronic Lymphocytic Leukemia. *N. Engl. J. Med.* **2000**, *343*, 1750–1757. [CrossRef] [PubMed]
26. Frank, D.A.; Mahajan, S.; Ritz, J. Fludarabine-Induced Immunosuppression Is Associated with Inhibition of STAT1 Signaling. *Nat. Med.* **1999**, *5*, 444–447. [CrossRef] [PubMed]
27. Hu, J.; Liu, Y.-F.; Wu, C.-F.; Xu, F.; Shen, Z.-X.; Zhu, Y.-M.; Li, J.-M.; Tang, W.; Zhao, W.-L.; Wu, W.; et al. Long-Term Efficacy and Safety of All-Trans Retinoic Acid/Arsenic Trioxide-Based Therapy in Newly Diagnosed Acute Promyelocytic Leukemia. *Proc. Natl. Acad. Sci. USA* **2009**, *106*, 3342–3347. [CrossRef]
28. Engels, F.K.; ten Tije, A.J.; Baker, S.D.; Lee, C.K.K.; Loos, W.J.; Vulto, A.G.; Verweij, J.; Sparreboom, A. Effect of Cytochrome P450 3A4 Inhibition on the Pharmacokinetics of Docetaxel. *Clin. Pharmacol. Ther.* **2004**, *75*, 448–454. [CrossRef]
29. Engels, F.K.; Sparreboom, A.; Mathot, R.A.A.; Verweij, J. Potential for Improvement of Docetaxel-Based Chemotherapy: A Pharmacological Review. *Br. J. Cancer* **2005**, *93*, 173–177. [CrossRef]
30. Shin, H.J.; Kim, D.N.; Lee, S.K. Association between Epstein-Barr Virus Infection and Chemoresistance to Docetaxel in Gastric Carcinoma. *Mol. Cells* **2011**, *32*, 173–179. [CrossRef]
31. Fei, X.F.; Wang, B.X.; Li, T.J.; Tashiro, S.; Minami, M.; Xing, D.J.; Ikejima, T. Evodiamine, a Constituent of Evodiae Fructus, Induces Anti-Proliferating Effects in Tumor Cells. *Cancer Sci.* **2003**, *94*, 92–98. [CrossRef]
32. Jiang, J.; Hu, C. Evodiamine: A Novel Anti-Cancer Alkaloid from Evodia Rutaecarpa. *Molecules* **2009**, *14*, 1852–1859. [CrossRef]
33. Choi, Y.H.; Shin, E.M.; Kim, Y.S.; Cai, X.F.; Lee, J.J.; Kim, H.P. Anti-Inflammatory Principles from the Fruits of Evodia Rutaecarpa and Their Cellular Action Mechanisms. *Arch. Pharm. Res.* **2006**, *29*, 293–297. [CrossRef] [PubMed]
34. Dai, J.-P.; Li, W.-Z.; Zhao, X.-F.; Wang, G.-F.; Yang, J.-C.; Zhang, L.; Chen, X.-X.; Xu, Y.-X.; Li, K.-S. A Drug Screening Method Based on the Autophagy Pathway and Studies of the Mechanism of Evodiamine against Influenza A Virus. *PLoS ONE* **2012**, *7*, e42706. [CrossRef] [PubMed]
35. Majnooni, M.B.; Fakhri, S.; Bahrami, G.; Naseri, M.; Farzaei, M.H.; Echeverría, J. Alkaloids as Potential Phytochemicals against SARS-CoV-2: Approaches to the Associated Pivotal Mechanisms. *Evid. Based Complement. Altern. Med.* **2021**, *2021*, e6632623. [CrossRef] [PubMed]
36. Vidoni, C.; Fuzimoto, A.; Ferraresi, A.; Isidoro, C. Targeting Autophagy with Natural Products to Prevent SARS-CoV-2 Infection. *J. Tradit. Complement. Med.* **2021**. [CrossRef]
37. Chen, X.; Zhou, S.; Li, H. Evodiamine Alleviates Severe Pneumonia Induced by Methicillin-Susceptible Staphylococcus Aureus Following Cytomegalovirus Reactivation through Suppressing NF-KB and MAPKs. *Int. J. Mol. Med.* **2018**, *42*, 3247–3255. [CrossRef]
38. Cho, K.-J.; Park, J.-H.; Hancock, J.F. Staurosporine. *Commun. Integr. Biol.* **2013**, *6*, e24746. [CrossRef]
39. Malsy, M.; Bitzinger, D.; Graf, B.; Bundscherer, A. Staurosporine Induces Apoptosis in Pancreatic Carcinoma Cells PaTu 8988t and Panc-1 via the Intrinsic Signaling Pathway. *Eur. J. Med. Res.* **2019**, *24*, 5. [CrossRef]
40. Omura, S.; Sasaki, Y.; Iwai, Y.; Takeshima, H. Staurosporine, a Potentially Important Gift from a Microorganism. *J. Antibiot.* **1995**, *48*, 535–548. [CrossRef]
41. Szkudelska, K.; Szkudelski, T. Resveratrol, Obesity and Diabetes. *Eur. J. Pharmacol.* **2010**, *635*, 1–8. [CrossRef]
42. Das, S.; Das, D.K. Anti-Inflammatory Responses of Resveratrol. *Inflamm. Allergy Drug Targets Discontin.* **2022**, *6*, 168–173. [CrossRef]
43. Elmali, N.; Baysal, O.; Harma, A.; Esenkaya, I.; Mizrak, B. Effects of Resveratrol in Inflammatory Arthritis. *Inflammation* **2007**, *30*, 1–6. [CrossRef] [PubMed]
44. Berman, A.Y.; Motechin, R.A.; Wiesenfeld, M.Y.; Holz, M.K. The Therapeutic Potential of Resveratrol: A Review of Clinical Trials. *Npj Precis. Oncol.* **2017**, *1*, 1–9. [CrossRef]
45. Anekonda, T.S. Resveratrol—A Boon for Treating Alzheimer's Disease? *Brain Res. Rev.* **2006**, *52*, 316–326. [CrossRef] [PubMed]
46. Filip, V.; Plocková, M.; Šmidrkal, J.; Špičková, Z.; Melzoch, K.; Schmidt, Š. Resveratrol and Its Antioxidant and Antimicrobial Effectiveness. *Food Chem.* **2003**, *83*, 585–593. [CrossRef]
47. Campagna, M.; Rivas, C. Antiviral Activity of Resveratrol. *Biochem. Soc. Trans.* **2010**, *38*, 50–53. [CrossRef] [PubMed]
48. Bradamante, S.; Barenghi, L.; Villa, A. Cardiovascular Protective Effects of Resveratrol. *Cardiovasc. Drug Rev.* **2004**, *22*, 169–188. [CrossRef]
49. Daniel, E.; Aylwin, S.; Mustafa, O.; Ball, S.; Munir, A.; Boelaert, K.; Chortis, V.; Cuthbertson, D.J.; Daousi, C.; Rajeev, S.P.; et al. Effectiveness of Metyrapone in Treating Cushing's Syndrome: A Retrospective Multicenter Study in 195 Patients. *J. Clin. Endocrinol. Metab.* **2015**, *100*, 4146–4154. [CrossRef]
50. Jahn, H.; Schick, M.; Kiefer, F.; Kellner, M.; Yassouridis, A.; Wiedemann, K. Metyrapone as Additive Treatment in Major Depression: A Double-Blind and Placebo-Controlled Trial. *Arch. Gen. Psychiatry* **2004**, *61*, 1235–1244. [CrossRef]

51. Filippakopoulos, P.; Qi, J.; Picaud, S.; Shen, Y.; Smith, W.B.; Fedorov, O.; Morse, E.M.; Keates, T.; Hickman, T.T.; Felletar, I.; et al. Selective Inhibition of BET Bromodomains. *Nature* **2010**, *468*, 1067–1073. [CrossRef]

52. Gibbons, H.R.; Mi, D.J.; Farley, V.M.; Esmond, T.; Kaood, M.B.; Aune, T.M. Bromodomain Inhibitor JQ1 Reversibly Blocks IFN-γ Production. *Sci. Rep.* **2019**, *9*, 10280. [CrossRef]

53. Delmore, J.E.; Issa, G.C.; Lemieux, M.E.; Rahl, P.B.; Shi, J.; Jacobs, H.M.; Kastritis, E.; Gilpatrick, T.; Paranal, R.M.; Qi, J.; et al. BET Bromodomain Inhibition as a Therapeutic Strategy to Target C-Myc. *Cell* **2011**, *146*, 904–917. [CrossRef] [PubMed]

54. Baratta, M.G.; Schinzel, A.C.; Zwang, Y.; Bandopadhayay, P.; Bowman-Colin, C.; Kutt, J.; Curtis, J.; Piao, H.; Wong, L.C.; Kung, A.L.; et al. An In-Tumor Genetic Screen Reveals That the BET Bromodomain Protein, BRD4, Is a Potential Therapeutic Target in Ovarian Carcinoma. *Proc. Natl. Acad. Sci. USA* **2015**, *112*, 232–237. [CrossRef] [PubMed]

55. Mu, J.; Zhang, D.; Tian, Y.; Xie, Z.; Zou, M.-H. BRD4 Inhibition by JQ1 Prevents High-Fat Diet-Induced Diabetic Cardiomyopathy by Activating PINK1/Parkin-Mediated Mitophagy In Vivo. *J. Mol. Cell. Cardiol.* **2020**, *149*, 1–14. [CrossRef] [PubMed]

56. Stratton, M.S.; Bagchi, R.A.; Felisbino, M.B.; Hirsch, R.A.; Smith, H.E.; Riching, A.S.; Enyart, B.Y.; Koch, K.A.; Cavasin, M.A.; Alexanian, M.; et al. Dynamic Chromatin Targeting of BRD4 Stimulates Cardiac Fibroblast Activation. *Circ. Res.* **2019**, *125*, 662–677. [CrossRef] [PubMed]

57. Meng, S.; Zhang, L.; Tang, Y.; Tu, Q.; Zheng, L.; Yu, L.; Murray, D.; Cheng, J.; Kim, S.H.; Zhou, X.; et al. BET Inhibitor JQ1 Blocks Inflammation and Bone Destruction. *J. Dent. Res.* **2014**, *93*, 657–662. [CrossRef]

58. Leoni, F.; Fossati, G.; Lewis, E.C.; Lee, J.-K.; Porro, G.; Pagani, P.; Modena, D.; Moras, M.L.; Pozzi, P.; Reznikov, L.L.; et al. The Histone Deacetylase Inhibitor ITF2357 Reduces Production of Pro-Inflammatory Cytokines In Vitro and Systemic Inflammation In Vivo. *Mol. Med.* **2005**, *11*, 1–15. [CrossRef]

59. Milan, M.; Pace, V.; Maiullari, F.; Chirivì, M.; Baci, D.; Maiullari, S.; Madaro, L.; Maccari, S.; Stati, T.; Marano, G.; et al. Givinostat Reduces Adverse Cardiac Remodeling through Regulating Fibroblasts Activation. *Cell Death Dis.* **2018**, *9*, 1–17. [CrossRef]

60. Tambaro, F.P.; Dell'Aversana, C.; Carafa, V.; Nebbioso, A.; Radic, B.; Ferrara, F.; Altucci, L. Histone Deacetylase Inhibitors: Clinical Implications for Hematological Malignancies. *Clin. Epigenet.* **2010**, *1*, 25–44. [CrossRef]

61. Jaskulska, A.; Janecka, A.E.; Gach-Janczak, K. Thapsigargin—From Traditional Medicine to Anticancer Drug. *Int. J. Mol. Sci.* **2020**, *22*, 4. [CrossRef]

62. Sehgal, P.; Szalai, P.; Olesen, C.; Praetorius, H.A.; Nissen, P.; Christensen, S.B.; Engedal, N.; Møller, J.V. Inhibition of the Sarco/Endoplasmic Reticulum (ER) Ca^{2+}-ATPase by Thapsigargin Analogs Induces Cell Death via ER Ca^{2+} Depletion and the Unfolded Protein Response. *J. Biol. Chem.* **2017**, *292*, 19656–19673. [CrossRef]

63. Al-Beltagi, S.; Preda, C.A.; Goulding, L.V.; James, J.; Pu, J.; Skinner, P.; Jiang, Z.; Wang, B.L.; Yang, J.; Banyard, A.C.; et al. Thapsigargin Is a Broad-Spectrum Inhibitor of Major Human Respiratory Viruses: Coronavirus, Respiratory Syncytial Virus and Influenza A Virus. *Viruses* **2021**, *13*, 234. [CrossRef]

64. Goulding, L.V.; Yang, J.; Jiang, Z.; Zhang, H.; Lea, D.; Emes, R.D.; Dottorini, T.; Pu, J.; Liu, J.; Chang, K.-C. Thapsigargin at Non-Cytotoxic Levels Induces a Potent Host Antiviral Response That Blocks Influenza A Virus Replication. *Viruses* **2020**, *12*, 1093. [CrossRef]

65. Ayaz, S.I.; Sharkey, C.M.; Kwiatkowski, G.M.; Wilson, S.S.; John, R.S.; Tolomello, R.; Mahajan, A.; Millis, S.; Levy, P.D. Intravenous Enalaprilat for Treatment of Acute Hypertensive Heart Failure in the Emergency Department. *Int. J. Emerg. Med.* **2016**, *9*, 28. [CrossRef] [PubMed]

66. Pandey, K.K. Critical Appraisal of Elvitegravir in the Treatment of HIV-1/AIDS. *HIVAIDS* **2014**, *6*, 81–90. [CrossRef] [PubMed]

67. Schafer, J.J.; Squires, K.E. Integrase Inhibitors: A Novel Class of Antiretroviral Agents. *Ann. Pharmacother.* **2010**, *44*, 145–156. [CrossRef]

68. Li, P.; Dorsch, W.; Lauffer, D.J.; Bilimoria, D.; Chauret, N.; Court, J.J.; Das, S.K.; Denis, F.; Mani, N.; Nanthakumar, S.; et al. Discovery of Novel Allosteric HCV NS5B Inhibitors. 2. Lactam-Containing Thiophene Carboxylates. *ACS Med. Chem. Lett.* **2017**, *8*, 251–255. [CrossRef] [PubMed]

69. Abdurakhmanov, E.; Øie Solbak, S.; Danielson, U.H. Biophysical Mode-of-Action and Selectivity Analysis of Allosteric Inhibitors of Hepatitis C Virus (HCV) Polymerase. *Viruses* **2017**, *9*, 151. [CrossRef]

70. Mohamed, K.; Yazdanpanah, N.; Saghazadeh, A.; Rezaei, N. Computational Drug Discovery and Repurposing for the Treatment of COVID-19: A Systematic Review. *Bioorg. Chem.* **2021**, *106*, 104490. [CrossRef]

71. Parashar, D.; Paingankar, M.S.; Kumar, S.; Gokhale, M.D.; Sudeep, A.B.; Shinde, S.B.; Arankalle, V.A. Administration of E2 and NS1 SiRNAs Inhibit Chikungunya Virus Replication in Vitro and Protects Mice Infected with the Virus. *PLoS Negl. Trop. Dis.* **2013**, *7*, e2405. [CrossRef]

72. Patil, P.; Agrawal, M.; Almelkar, S.; Jeengar, M.K.; More, A.; Alagarasu, K.; Kumar, N.V.; Mainkar, P.S.; Parashar, D.; Cherian, S. In Vitro and In Vivo Studies Reveal α-Mangostin, a Xanthonoid from Garcinia Mangostana, as a Promising Natural Antiviral Compound against Chikungunya Virus. *Virol. J.* **2021**, *18*, 47. [CrossRef]

73. Panda, K.; Alagarasu, K.; Patil, P.; Agrawal, M.; More, A.; Kumar, N.V.; Mainkar, P.S.; Parashar, D.; Cherian, S. In Vitro Antiviral Activity of α-Mangostin against Dengue Virus Serotype-2 (DENV-2). *Molecules* **2021**, *26*, 3016. [CrossRef] [PubMed]

74. Kim, S.; Thiessen, P.A.; Bolton, E.E.; Chen, J.; Fu, G.; Gindulyte, A.; Han, L.; He, J.; He, S.; Shoemaker, B.A.; et al. PubChem Substance and Compound Databases. *Nucleic Acids Res.* **2016**, *44*, D1202–D1213. [CrossRef] [PubMed]

75. Berman, H.M.; Westbrook, J.; Feng, Z.; Gilliland, G.; Bhat, T.N.; Weissig, H.; Shindyalov, I.N.; Bourne, P.E. The Protein Data Bank. *Nucleic Acids Res.* **2000**, *28*, 235–242. [CrossRef]

76. Friesner, R.A.; Banks, J.L.; Murphy, R.B.; Halgren, T.A.; Klicic, J.J.; Mainz, D.T.; Repasky, M.P.; Knoll, E.H.; Shelley, M.; Perry, J.K.; et al. Glide: A New Approach for Rapid, Accurate Docking and Scoring. 1. Method and Assessment of Docking Accuracy. *J. Med. Chem.* **2004**, *47*, 1739–1749. [CrossRef]

77. Halgren, T.A.; Murphy, R.B.; Friesner, R.A.; Beard, H.S.; Frye, L.L.; Pollard, W.T.; Banks, J.L. Glide: A New Approach for Rapid, Accurate Docking and Scoring. 2. Enrichment Factors in Database Screening. *J. Med. Chem.* **2004**, *47*, 1750–1759. [CrossRef] [PubMed]

78. Modis, Y.; Ogata, S.; Clements, D.; Harrison, S.C. A Ligand-Binding Pocket in the Dengue Virus Envelope Glycoprotein. *Proc. Natl. Acad. Sci. USA* **2003**, *100*, 6986–6991. [CrossRef]

79. Yildiz, M.; Ghosh, S.; Bell, J.A.; Sherman, W.; Hardy, J.A. Allosteric Inhibition of the NS2B-NS3 Protease from Dengue Virus. *ACS Chem. Biol.* **2013**, *8*, 2744–2752. [CrossRef]

80. El Sahili, A.; Soh, T.S.; Schiltz, J.; Gharbi-Ayachi, A.; Seh, C.C.; Shi, P.-Y.; Lim, S.P.; Lescar, J. NS5 from Dengue Virus Serotype 2 Can Adopt a Conformation Analogous to That of Its Zika Virus and Japanese Encephalitis Virus Homologues. *J. Virol.* **2019**, *94*, e01294-19. [CrossRef]

81. Ayala-Nuñez, N.V.; Jarupathirun, P.; Kaptein, S.J.F.; Neyts, J.; Smit, J.M. Antibody-Dependent Enhancement of Dengue Virus Infection Is Inhibited by SA-17, a Doxorubicin Derivative. *Antiviral Res.* **2013**, *100*, 238–245. [CrossRef]

82. Guzman, M.G.; Vazquez, S. The Complexity of Antibody-Dependent Enhancement of Dengue Virus Infection. *Viruses* **2010**, *2*, 2649–2662. [CrossRef]

83. Fried, J.R.; Gibbons, R.V.; Kalayanarooj, S.; Thomas, S.J.; Srikiatkhachorn, A.; Yoon, I.-K.; Jarman, R.G.; Green, S.; Rothman, A.L.; Cummings, D.A.T. Serotype-Specific Differences in the Risk of Dengue Hemorrhagic Fever: An Analysis of Data Collected in Bangkok, Thailand from 1994 to 2006. *PLoS Negl. Trop. Dis.* **2010**, *4*, e617. [CrossRef] [PubMed]

84. Malakar, S.; Sreelatha, L.; Dechtawewat, T.; Noisakran, S.; Yenchitsomanus, P.; Chu, J.J.H.; Limjindaporn, T. Drug Repurposing of Quinine as Antiviral against Dengue Virus Infection. *Virus Res.* **2018**, *255*, 171–178. [CrossRef] [PubMed]

85. Paemanee, A.; Hitakarun, A.; Roytrakul, S.; Smith, D.R. Screening of Melatonin, α-Tocopherol, Folic Acid, Acetyl-l-Carnitine and Resveratrol for Anti-Dengue 2 Virus Activity. *BMC Res. Notes* **2018**, *11*, 307. [CrossRef] [PubMed]

86. Kato, F.; Ishida, Y.; Oishi, S.; Fujii, N.; Watanabe, S.; Vasudevan, S.G.; Tajima, S.; Takasaki, T.; Suzuki, Y.; Ichiyama, K.; et al. Novel Antiviral Activity of Bromocriptine against Dengue Virus Replication. *Antiviral Res.* **2016**, *131*, 141–147. [CrossRef] [PubMed]

87. Shen, T.-J.; Hanh, V.T.; Nguyen, T.Q.; Jhan, M.-K.; Ho, M.-R.; Lin, C.-F. Repurposing the Antiemetic Metoclopramide as an Antiviral against Dengue Virus Infection in Neuronal Cells. *Front. Cell. Infect. Microbiol.* **2021**, *10*, 606743. [CrossRef]

88. Zainal, N.; Chang, C.-P.; Cheng, Y.-L.; Wu, Y.-W.; Anderson, R.; Wan, S.-W.; Chen, C.-L.; Ho, T.-S.; AbuBakar, S.; Lin, Y.-S. Resveratrol Treatment Reveals a Novel Role for HMGB1 in Regulation of the Type 1 Interferon Response in Dengue Virus Infection. *Sci. Rep.* **2017**, *7*, 42998. [CrossRef]

89. Chatterjee, K.; Zhang, J.; Honbo, N.; Karliner, J.S. Doxorubicin Cardiomyopathy. *Cardiology* **2010**, *115*, 155–162. [CrossRef]

90. Smeets, N.J.L.; Schreuder, M.F.; Dalinghaus, M.; Male, C.; Lagler, F.B.; Walsh, J.; Laer, S.; de Wildt, S.N. Pharmacology of Enalapril in Children: A Review. *Drug Discov. Today* **2020**, *25*, 1957–1970. [CrossRef]

91. Hernández-Fonseca, J.P.; Durán, A.; Valero, N.; Mosquera, J. Losartan and Enalapril Decrease Viral Absorption and Interleukin 1 Beta Production by Macrophages in an Experimental Dengue Virus Infection. *Arch. Virol.* **2015**, *160*, 2861–2865. [CrossRef]

92. Loe, M.W.C.; Lee, R.C.H.; Chu, J.J.H. Antiviral Activity of the FDA-Approved Drug Candesartan Cilexetil against Zika Virus Infection. *Antiviral Res.* **2019**, *172*, 104637. [CrossRef]